

# Raman and FTIR spectroscopy of natural oxalates: Implications for the evidence of life on Mars

R. L. Frost<sup>1</sup>, YANG Jing<sup>2</sup> & Zhe Ding<sup>1</sup>

1. Inorganic Materials Research Program, Queensland University of Technology, 2 George Street, Brisbane, GPO Box 2434, Queensland 4001, Australia;

2. School of Materials, China University of Geosciences, Beijing 100083, China

Correspondence should be addressed to R. L. Frost (e-mail: r.frost@qut.edu.au)

**Abstract** Evidence for the existence of primitive life forms such as lichens and fungi can be based upon the formation of oxalates. Oxalates are most readily detected using Raman spectroscopy. A comparative study of a suite of natural oxalates including weddellite, whewellite, moolooite, humboldtine, glushinskite, natroxalate and oxammite has been undertaken using Raman spectroscopy. The minerals are characterised by the Raman position of the CO stretching vibration which is cation sensitive. The band is observed at 1468 cm<sup>-1</sup> for weddellite, 1489 cm<sup>-1</sup> for moolooite, 1471 cm<sup>-1</sup> for glushinskite and 1456 cm<sup>-1</sup> for natroxalate. Except for oxammite, the infrared and Raman spectra are mutually exclusive indicating the minerals are bidentate. Differences are also observed in the water OH stretching bands of the minerals. The significance of this work rests with the ability of Raman spectroscopy to identify oxalates which often occur as a film on a host rock. As such Raman spectroscopy has the potential to identify the existence or pre-existence of life forms on planets such as Mars.

**Keywords:** oxalate, weddellite, moolooite, humboldtine, natroxalate, oxammite, glushinskite.

**DOI:** 10.1360/03wd0145

The presence of oxalates is widespread in nature. These minerals form as the result of expulsion of heavy metals from fungi, lichens and plants<sup>[1–3]</sup>. The production of simple organic acids such as oxalic and citric acids has profound implications for metal speciation in biogeochemical cycles<sup>[4]</sup>. The metal complexing properties of the acids are essential to the nutrition of fungi and lichens and affect the metal stability and mobility in the environment<sup>[4]</sup>. Lichens and fungi produce the oxalates of heavy metals as a mechanism for the removal of heavy metals from the plant<sup>[5]</sup>. The presence of these oxalate crystals appears to have an effect similar to that found in cacti<sup>[6]</sup>. Among the oxalates are the two calcium oxalates known as weddellite (the dihydrate) and whewellite (monohydrate). Ca-oxalate exists in two well-described modifications: as the more stable monoclinic monohydrate whew-

ellite and the less stable tetragonal dihydrate weddellite. Weddellite serves for lichens as a water absorbing and accumulating substrate which transforms to whewellite when humidity drops. Such minerals are important in human physiology as the minerals are found in urinary tracts<sup>[7,8]</sup>. Many other divalent oxalates exist in nature. The magnesium based oxalate is known as glushinskite<sup>[9,10]</sup>. The copper oxalate is known as moolooite<sup>[2,11]</sup> and the ferrous oxalate as humboldtine<sup>[12,13]</sup>. These three oxalates are also the product of lichen growth. Two natural univalent oxalates are known. These are the oxalates of sodium and ammonium known as natroxalate and oxammite<sup>[14]</sup>.

Indeed the presence of oxalates has been evidence for the deterioration of works of art<sup>[15–17]</sup>. Carbon dating of oxalic acid enables estimates of the age of the works of art<sup>[18]</sup>. The presence of the oxalates has been used as indicators of climate change<sup>[19]</sup>. The presence of pigments in ancient works of art effected the growth of lichens on the art works<sup>[20]</sup>. In calcareous artifacts such as the famous Chinese terra cotta soldiers or Egyptian epigraphs they lead to a destruction of the surface by forming Ca-oxalate layers and thus to a deterioration of the historical work of art. But in places where the surface is covered by some blue colours (Egyptian and Chinese Blue, Chinese Purple) the growth of lichens is inhibited and the artifacts are well preserved. The copper ion contained in the pigments is responsible for this effect since copper is a strong poison for micro-organisms<sup>[20]</sup>. Weddellite and whewellite very often occur together with gypsum on the surface of calcareous artifacts exposed in the mediterranean urban environment, as main constituents of reddish patinas called in Italy “scialbatura”. The origin of this is a matter of controversy. The observation of the interface between calcite substratum and the above mentioned secondary minerals is an important step in the explanation of alteration process of artifacts of historic and artistic interest<sup>[21]</sup>. Studies of the black paint have shown the presence of oxalates in the paint with serious implications for remediation<sup>[22]</sup>. The use of infrared and Raman spectroscopy for the study of oxalates originated with the necessity to study renal stones<sup>[23,24]</sup>. FT Raman spectroscopy has been used to study urolithiasis disease that has been studied for many years, and the ethiopathogenesis of stone formation is not well understood<sup>[25]</sup>.

Whilst there have been several studies of synthetic metal oxalates<sup>[26–32]</sup>, few studies of natural oxalates have been forthcoming and no comprehensive comparison of the natural oxalates has been undertaken. Few studies of the spectroscopy of water in these minerals have been forthcoming. The objective of this work is to undertake a comparative study using a combination of Raman and infrared spectroscopy of a suite of common natural oxalates.

## 1 Experimental

(i) Minerals. Weddellite, originated from the Weddell Sea, Antarctica. Whewellite, registered sample number M5531 originated from Burg River, near Dresden, Saxony, Germany. Moolooite, originated from Murchison, Mooloo Downs Station, Western Australia. Humboldtine, sample number M13748, originated from Bohemia, Czech Republic. Glusinskite, originated from Lena coal basin, Yakutia, Siberia, Russia. Natroxolate, sample number M46430, originated from Alluaiv Mtn., Lovozero Massif, Kola Peninsula, Russia. Oxammite, originated from Guanape Island, Peru. The samples were phase analyzed using X-ray diffraction and the compositions checked using EDX measurements.

(ii) Raman microprobe spectroscopy. The crystals of the oxalate minerals were placed and orientated on the stage of an Olympus BHSM microscope, equipped with 10× and 50× objectives and part of a Renishaw 1000 Raman microscope system, which also includes a monochromator, a filter system and a charge coupled device (CCD). Raman spectra were excited by a Nd-Yag laser (780 nm) at a resolution of 2 cm<sup>-1</sup> in the range between 100 and 4000 cm<sup>-1</sup>. It should be noted that the limitations of the detector prevent the collection of data at wavenumbers above 3000 cm<sup>-1</sup> Raman shift. Repeated acquisition using the highest magnification were accumulated to improve the signal to noise ratio. Spectra were calibrated using the 520.5 cm<sup>-1</sup> line of a silicon wafer. In order to ensure that the correct spectra are obtained, the incident excitation radiation was scrambled.

Spectroscopic manipulation such as baseline adjustment, smoothing and normalisation were performed using the Spectralcalc software package GRAMS (Galactic Industries Corporation, NH, USA). Band component analysis was undertaken using the Jandel "Peakfit" software package, which enabled the type of fitting, function to be selected and allows specific parameters to be fixed or varied accordingly. Band fitting was done using a Gauss-Lorentz cross-product function with the minimum number of component bands used for the fitting process. The Gauss-Lorentz ratio was maintained at values greater than 0.7 and fitting was undertaken until reproducible results were obtained with squared correlations of  $r^2$  greater than 0.995.

## 2 Results and discussion

(i) Factor group analysis. Aqueous oxalate is uncoordinated and will be of point group D<sub>2d</sub>. Thus the vibrational activity is given by  $G = 3A_1 + B_1 + 2B_1 + 3E$ . Thus all modes are Raman active and the  $2B_1 + 3E$  modes are infrared active. All oxygens in the structure are equivalent and hence only one symmetric stretching mode should occur. Upon coordination of the oxalate as a mono-

oxalato species as will occur in the natural minerals, the symmetry species is reduced to C<sub>2v</sub>. The irreducible expression is then given by  $G = 6A_1 + 2A_2 + 5B_1 + 2B_2$ . Hence all modes are both Raman and infrared active. In this situation both the symmetric and antisymmetric stretching modes will be observed. If two moles of oxalate are bonded to the cation then the molecular point group will be D<sub>2h</sub> and the irreducible representation is given by  $G = 7A_g + 3B_{1g} + 3B_{2g} + 5B_{3g} + 3A_u + 7B_{1u} + 7B_{2u} + 4B_{3u}$ . The first four modes are Raman active (namely  $7A_g + 3B_{1g} + 3B_{2g} + 5B_{3g}$ ) and the last four modes are infrared active (namely  $3A_u + 7B_{1u} + 7B_{2u} + 4B_{3u}$ ). Under this symmetry, there is a centre of symmetry which means the infrared and Raman bands are exclusive.

(ii) Raman spectra of the CO stretching region.

The Raman spectra of the 1200–1800 cm<sup>-1</sup> region is shown in Fig. 1. The results of the Raman spectroscopic analysis together with the band assignments is given in Table 1. A band is identified in all the spectra in the 1456–1473 cm<sup>-1</sup> range and is assigned to the  $\nu(C-O)$  stretching mode. The position of this band was identified at 1449 cm<sup>-1</sup> for potassium oxalate in the solid state<sup>[29]</sup>. For weddellite and humboldtine the band was observed at 1468

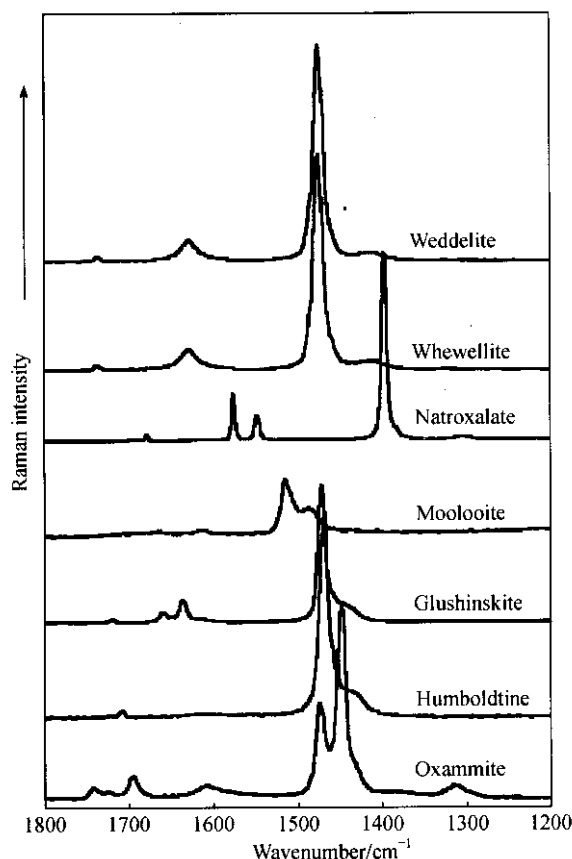


Fig. 1. Raman spectra of the 1200–1800 cm<sup>-1</sup> region.

cm<sup>-1</sup>. The position of the band for whewellite is the same as for weddellite. It is possible to discriminate between hydration states of calcium oxalate; the monohydrate (whewellite) featured a  $\nu_{(C=O)}$  stretching band at 1493 cm<sup>-1</sup> whereas the dihydrate (weddellite) had a contrasting  $\nu_{(C=O)}$  stretching band at 1475 cm<sup>-1</sup>. The band was observed for moolooite at 1489 cm<sup>-1</sup>. Moolooite is the bis - copper( II ) oxalate and the natural sample contains no water of hydration. Previous studies of the dihydrate copper( II ) oxalate observed the position at 1495 cm<sup>-1</sup>[29]. The Raman spectrum of the mineral glushinskite shows a band at 1471 cm<sup>-1</sup>. The spectrum for natroxalate shows a band at 1456 cm<sup>-1</sup>, a wavenumber position which is comparatively low compared with the other natural oxalates. Natroxalate is similar to that of moolooite in that no water of

crystallisation is found for the natural mineral.

The Raman spectra of many of the minerals show additional bands on the low wavenumber side of the symmetric stretching mode. Bands are observed at 1411 cm<sup>-1</sup> for weddellite and whewellite, 1433 cm<sup>-1</sup> for moolooite, 1450 cm<sup>-1</sup> for humboldtine and 1454 cm<sup>-1</sup> for glushinskite. For oxammite a number of additional bands are observed at 1451, 1447 and 1430 cm<sup>-1</sup>. It is suspected that these additional bands are also assignable to the symmetric stretching modes; but of molecular species other than the bis-oxalate complexes. Another possibility is that these bands are due to the B<sub>2g</sub> mode, which is the O—C=O wag. The position of this band is identified at 1392 cm<sup>-1</sup> for aqueous potassium oxalate and at 1348 cm<sup>-1</sup> for potassium oxalate in the solid state<sup>[33,35]</sup>. A band

Table 1 Raman spectroscopic analysis of oxalates minerals

Ca (weddellite)	Cu (moolooite)	Fe <sup>2+</sup> (humboldtine)	Mg (glushinskite)	Na (natroxalate)	NH <sub>4</sub> (oxammite)	Infrared <sup>[41]</sup>	Band assignment
3467		3315	3391		3235		OH stretching
3266			3367		3030		
			3254				
					2995		NH stretching
					2900		
					2879		
					2161		
					1902		
1737	1673	1708	1720	1750	1737		
1628	1614	1555	1660	1643	1695	1632	$\nu_{(C=O)}$
			1636	1614	1605		
			1612				
1475	1514						$\nu_{(C=O)}$
1468	1489	1468	1471	1456	1473	1433	$\nu_{(C-O)} + \nu_{(C-C)}$
					1451		
					1447		
					1430		
1411	1433	1450	1454	1358	1417	1302	$\nu_{(C-O)} + \nu_{(O-C=O)}$
					1312		
1055	1120						
1053							
909	921	913	915		892	890	$\nu_{(C-C)} + \nu_{(O-C=O)}$
868	831	856	861	884	866		
				875	815		
			657		642	785	$\nu_{(O-C=O)} + \nu_{(M-O)}$
596	610	582	585	567		622	water libration
	584						
505	558	518	527			519	$\nu_{(M-O)} + \nu_{(C-C)}$
			521			519	ring deform + $\nu_{(O-C=O)}$
				481	489	428	$\nu_{(M-O)} + \text{ring deform}$
					438	419	
						377	$\nu_{(O-C=O)} + \nu_{(C-C)}$
						364	
259	290	293	310		278	291	out of plane bends
220	209	246	265		224		
			237				
			226				
188		203	221	221	210		
				156	198		
				117	181		
					160		

in this position is observed at  $1358\text{ cm}^{-1}$  for natroxalate. Bands are observed at  $1417$  and  $1312\text{ cm}^{-1}$  for oxammite, which may also be attributable to the  $\text{O}-\text{C}=\text{O}$  wag.

(iii) Infrared spectrum of the CO stretching region.

The infrared spectra of the suite of minerals is shown in Fig. 2. The results of the infrared spectral analysis are reported in Table 2. A comparison of Figs. 1 and 2 confirms the rule of mutual exclusion for the spectroscopy of these natural oxalates. No bands are observed in the infrared spectra round  $1460\text{ cm}^{-1}$  and no intense bands are observed in the Raman spectra around  $1600\text{ cm}^{-1}$ , although some low intensity bands may be observed in this region in Fig. 1. The exception is oxammite where bands are observed in both the Raman and infrared spectra around  $1400\text{ cm}^{-1}$ . For aqueous oxalate the antisymmetric stretching ( $B_{2u}$ ) mode is observed at  $1600\text{ cm}^{-1}$ . For weddellite and whewellite two bands are observed at  $1623$  and  $1605\text{ cm}^{-1}$ . The IR spectrum of humboldtine shows a single band centred at  $1615\text{ cm}^{-1}$ .

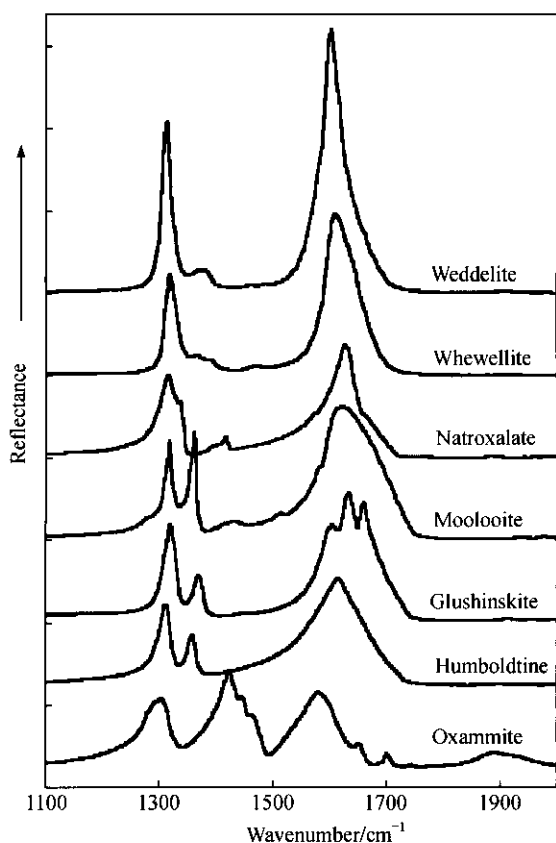


Fig. 2. Infrared spectra of the minerals.

For moolooite the band is observed at  $1632\text{ cm}^{-1}$  and is strongly asymmetric and component bands may be resolved at  $1722$ ,  $1679$ ,  $1632$  and  $1602\text{ cm}^{-1}$ . For glushinskite bands are observed at  $1679$ ,  $1660$ ,  $1634$  and  $1603$

$\text{cm}^{-1}$ . The IR spectrum of natroxalate shows bands at  $1675$ ,  $1628$  and  $1604\text{ cm}^{-1}$ . Published IR data suggests that there should be a single band at  $1632\text{ cm}^{-1}$ <sup>[29]</sup>. The reason for multiple antisymmetric stretching modes for each of the minerals is unclear; suffice to express that multiple species may be present. For example many oxalate minerals show polymerisation<sup>[33,34]</sup>. The mineral oxammite fits well into this category. Multiple bands are observed in the infrared spectrum for both the symmetric and antisymmetric stretching modes.

The infrared spectra show quite intense bands centred around  $1300\text{ cm}^{-1}$ . These bands may be assigned to  $B_{3u}$   $\text{O}-\text{C}=\text{O}$  stretching mode. For weddellite and whewellite bands are observed at  $1366$  and  $1309\text{ cm}^{-1}$ . For moolooite two intense bands are observed at  $1317$  and  $1361\text{ cm}^{-1}$  with low intensity bands at  $1352$ ,  $1311$  and  $1279\text{ cm}^{-1}$ . A band was observed at  $1365\text{ cm}^{-1}$  and assigned to the  $\text{O}-\text{C}=\text{O}$  stretching mode for synthetic copper(II) oxalate dihydrate<sup>[33,34]</sup>. Both humboldtine and glushinskite show a similar infrared pattern to moolooite with component bands at  $1312$  and  $1357$ ,  $1314$  and  $1369\text{ cm}^{-1}$  respectively. The IR spectrum of natroxalate shows strong intensity at  $1337$  and  $1314\text{ cm}^{-1}$  with low intensity bands at  $1416$ ,  $1400$ ,  $1296$  and  $1251\text{ cm}^{-1}$ . The infrared spectrum of oxammite shows bands at  $1288$  and  $1308\text{ cm}^{-1}$ . The reason for the multiplicity of bands cannot be attributed to a reduction of symmetry and loss of degeneracy but rather to the presence of multiple species. It is possible that not only the di-oxalate but the poly-oxalate, mono-oxalate and free oxalate are present in varying degrees of concentration.

(iv) Raman spectrum of the bending region. The Raman spectrum of the  $800-1100\text{ cm}^{-1}$  region is shown in Fig. 3. A Raman band is observed at around  $900\text{ cm}^{-1}$  and is assigned to the  $\nu(\text{C}-\text{O})$  stretching mode. The band is observed at  $909\text{ cm}^{-1}$  for weddellite,  $921\text{ cm}^{-1}$  for moolooite,  $913\text{ cm}^{-1}$  for humboldtine,  $915\text{ cm}^{-1}$  for glushinskite, and  $892\text{ cm}^{-1}$  for oxammite. The position for natroxalate is at  $884\text{ cm}^{-1}$  which corresponds well with the published value of  $888\text{ cm}^{-1}$  for solid potassium oxalate. It should be noted that there is a large shift ( $\sim 40\text{ cm}^{-1}$ ) for the  $\text{C}-\text{C}$  stretching vibration between the “free” oxalate and the oxalate in these natural oxalates. A second intense band for natroxalate is observed at  $875\text{ cm}^{-1}$ . This implies a non-equivalence of the  $\text{C}-\text{C}$  stretching vibrations. The Raman spectra of the oxalate minerals all show a low intensity band at around  $860\text{ cm}^{-1}$ . The band is observed at  $868\text{ cm}^{-1}$  for weddellite,  $833\text{ cm}^{-1}$  for moolooite,  $856\text{ cm}^{-1}$  for humboldtine,  $861\text{ cm}^{-1}$  for glushinskite, and  $866\text{ cm}^{-1}$  for oxammite. The band is assigned to the  $\text{O}-\text{C}=\text{O}$  bending mode. A band is not observed in this position for potassium oxalate.

Table 2 Infrared spectroscopic analysis of oxalates minerals

Ca (weddellite)	Cu (moolooite)	Fe <sup>2+</sup> (humboldtine)	Mg (glushinskite)	Na (natroxalate)	NH <sub>4</sub> (oxammite)	Infrared <sup>[41]</sup>	Band assignment
3593	3529	3472	3389		3195		OH stretching
3450	3347	3312	3380		3186		
3337	2971	3136	3360		3053		
3248			3305				
3089			3230				
			3126				NH stretching
					2978		
					2856		
					2840		
					2630		
					2344		1632 $\nu_{(C=O)}$
					1900		
1623	1722	1615	1679	1675	1701		
1605	1679		1660	1628	1651		
	1632		1634	1604	1582		
	1602		1603		1527		1500 $\nu_{(C=O)}$
	1574	1514	1580	1538			
	1543	1479					
	1512						1433 $\nu_{(C-O)} + \nu_{C-C}$
1399	1430				1466		
					1447		
					1425		1302 $\nu_{(C-O)} + d_{(O-C=O)}$
1366	1361	1357	1369	1416	1410		
1309	1352		1322	1400	1308		
	1317	1312	1314	1337	1288		
	1311	1301	1169	1314			
	1279	1266		1296			890 $\nu_{(C-C)} + d_{(O-C=O)}$
				1251			
917							
779	820	818	827	780	800	785	$(O-C=O) + \nu_{(M-O)}$
762	798	766	803	771	716		
		715		756			
601			684		635	622	water libration
					617		
						519	$\nu_{(M-O)} + \nu_{C-C}$
						519	ring deform + $d_{(O-C=O)}$
						428	$\nu_{(M-O)} + \text{ring deform}$
						419	
						377	$d_{(O-C=O)} + \nu_{C-C}$
						364	
						291	out of plane bends

( $\nu$ ) Infrared spectrum of the bending region. The infrared spectrum of the 500 to 1000  $\text{cm}^{-1}$  region is shown in Fig. 4. The first observation that can be made is that the  $C-C$  stretching mode is either not observed or is only weakly observed in the infrared spectrum. Two low intensity bands are observed at 884 and 957  $\text{cm}^{-1}$ . Whewellite shows only a single band at 917  $\text{cm}^{-1}$ . The IR spectrum of moolooite shows a very weak band at 917  $\text{cm}^{-1}$ . Humboldtine has a band at a similar position and oxammite a band at 871  $\text{cm}^{-1}$ . An intense band is observed for weddellite at 779  $\text{cm}^{-1}$  with a strong shoulder at 762  $\text{cm}^{-1}$ . The infrared spectrum of whewellite shows a broad band centred upon 820  $\text{cm}^{-1}$ . The IR spectrum of natroxalate shows

two strong bands at 818 and 766  $\text{cm}^{-1}$ . These bands are assigned to the  $O-C=O$  bending modes which are strong in the infrared spectrum and of low intensity in the Raman spectrum.

( $\nu$ ) Raman spectrum of the deformation modes of oxalate. The Raman spectrum of the low wavenumber region is shown in Fig. 5. Raman bands are observed for weddellite and whewellite at 596 and 505  $\text{cm}^{-1}$ . Natroxalate has Raman bands at 567 and 481  $\text{cm}^{-1}$ . The band at 596  $\text{cm}^{-1}$  is broad and of low intensity, and is attributed to water librational modes. The band at 505  $\text{cm}^{-1}$  for the calcium oxalates and at 481  $\text{cm}^{-1}$  for the sodium oxalate may be attributed to the symmetric  $O-C=O$  bending mode.

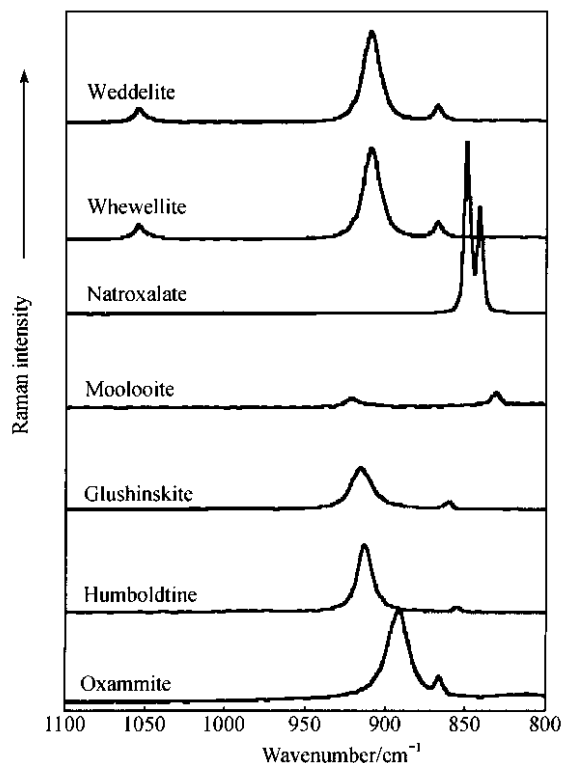


Fig. 3. Raman spectra of the 800–1100  $\text{cm}^{-1}$  region.

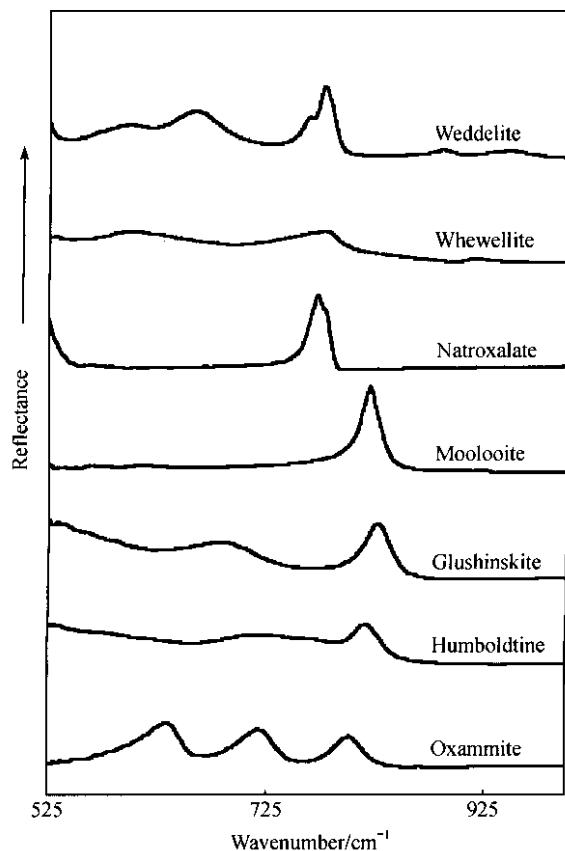


Fig. 4. Infrared spectrum of the 500–1000  $\text{cm}^{-1}$  region.

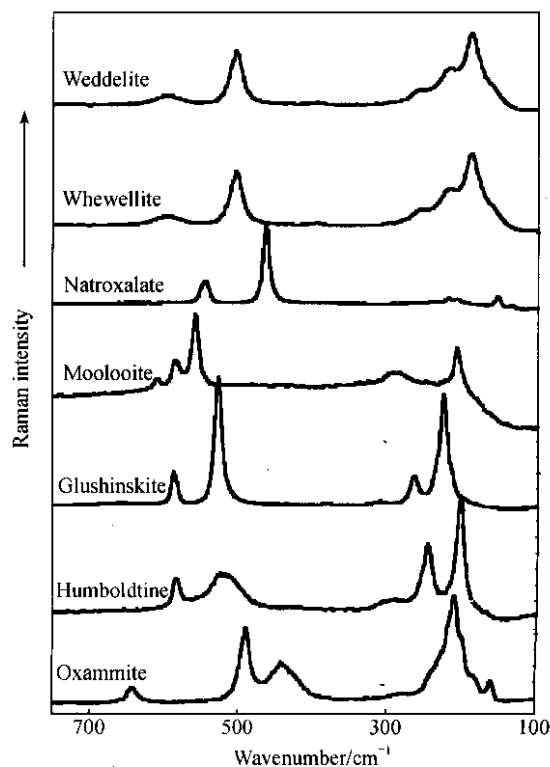


Fig. 5. Raman spectrum of the low wavenumber region.

For humboldtine the bands are observed at 582 and 518  $\text{cm}^{-1}$ . The Raman spectrum of moolooite shows more complexity with bands observed at 610, 584 and 558  $\text{cm}^{-1}$ . Such complexity was observed in the Raman spectrum of a synthetic copper(II) oxalate dihydrate<sup>[35]</sup>. In this work, Raman bands were observed at 616, 591, 563 and 498  $\text{cm}^{-1}$ . Raman bands were observed at 642, 489 and 438  $\text{cm}^{-1}$  for oxammite.

Fig. 5 also shows some quite intense bands in the 100–300  $\text{cm}^{-1}$  range. Both weddellite and whewellite show bands at 259, 220, 188 and 162  $\text{cm}^{-1}$ . One possible assignment is that the bands are due to CaO stretching and bending vibrations. The intensities of the bands for natroxalate are weak. For moolooite bands are observed at 209 and 290  $\text{cm}^{-1}$ . These bands may be assigned to the CuO stretching and bending modes respectively. The position of the bands differs slightly from that published for the copper(II) oxalate dihydrate<sup>[35]</sup>. Intense bands are observed for both glushinskite and humboldtine at 310, 265, 237 and 226  $\text{cm}^{-1}$ , and 293, 246 and 203  $\text{cm}^{-1}$  respectively. The Raman spectrum of oxammite is quite complex with multiple bands observed at 278, 224, 210, 198, 181 and 160  $\text{cm}^{-1}$ .

(vii) Raman spectrum of the OH stretching region.

It is interesting that many papers report the spectroscopy of oxalates but fail to mention the spectroscopy of

the water of crystallisation in the oxalate minerals. The Raman spectrum of the hydroxyl stretching region for the natural oxalates is shown in Fig. 6. Moolooite and natroxalate do not have any water of crystallisation and consequently no Raman spectrum of the OH stretching region is found. The Raman spectra of weddelite and whewellite are different in the OH stretching region. Two bands are observed for weddelite at 3467 and 3266  $\text{cm}^{-1}$  whereas bands are observed for whewellite at 3462, 3359, 3248 and 3067  $\text{cm}^{-1}$ . The Raman spectrum of the hydroxyl stretching region of glushinskite shows a sharp intense band at 3367  $\text{cm}^{-1}$  with low intensity bands at 3391 and 3254  $\text{cm}^{-1}$ . The raman spectrum of oxammite in this region shows complexity with the overlap of the OH and NH stretching vibrations. Two bands are observed at 3235 and 3030  $\text{cm}^{-1}$  and are assigned to the OH vibrations. Bands are observed at 2995, 2900 and 2879  $\text{cm}^{-1}$  and are attributed to the NH vibrational modes.

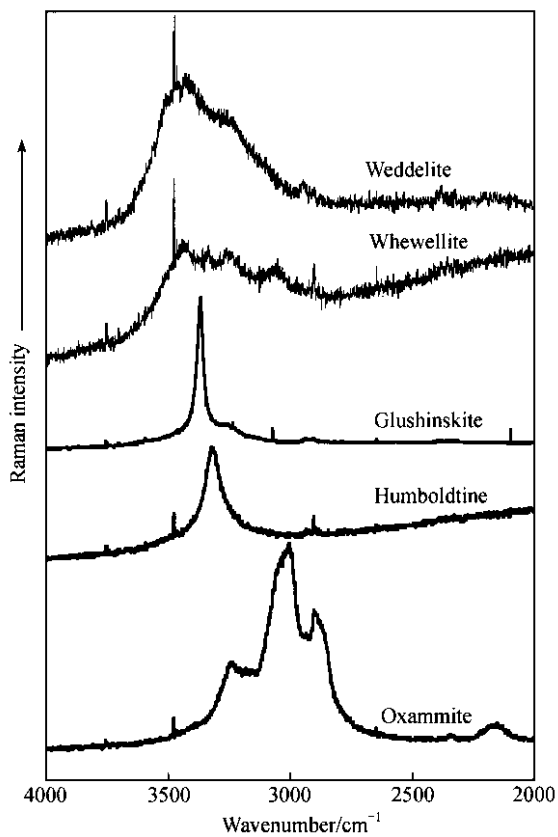


Fig. 6. Raman spectrum of the hydroxyl stretching region.

The patterns of the OH stretching vibrations observed in the Raman spectra are reflected in the infrared spectra (Fig. 7). The spectra of weddelite and whewellite are different. The infrared spectrum of weddelite shows OH stretching vibrations at 3593, 3450, 3337, 3248 and 3089  $\text{cm}^{-1}$ . The infrared spectra of whewellite shows a

broad pattern. No spectrum is observed for natroxalate and a low intensity broad band is observed for moolooite and in all probability represents adsorbed water. The infrared spectrum of glushinskite and humboldtine show intense bands at 3389 and 3472  $\text{cm}^{-1}$  respectively. Low intensity bands are observed for glushinskite at 3380, 3360, 3305, 3230 and 3126  $\text{cm}^{-1}$ . Low intensity bands are observed for humboldtine at 3312 and 3136  $\text{cm}^{-1}$ . In the case of oxammite infrared bands are observed at 3195, 3186 and 3053  $\text{cm}^{-1}$  and are attributed to the water OH stretching vibrations. The infrared bands observed at 2978, 2856, 2840, 2630 and 2344  $\text{cm}^{-1}$  are assigned to NH stretching vibrations. It is probable that the large number of bands observed in the NH stretching region is ascribed to the non-planar nature of oxammite<sup>[36]</sup>. It has been suggested that the oxalate is twisted around the C—C bond by some 28°<sup>[37]</sup>.

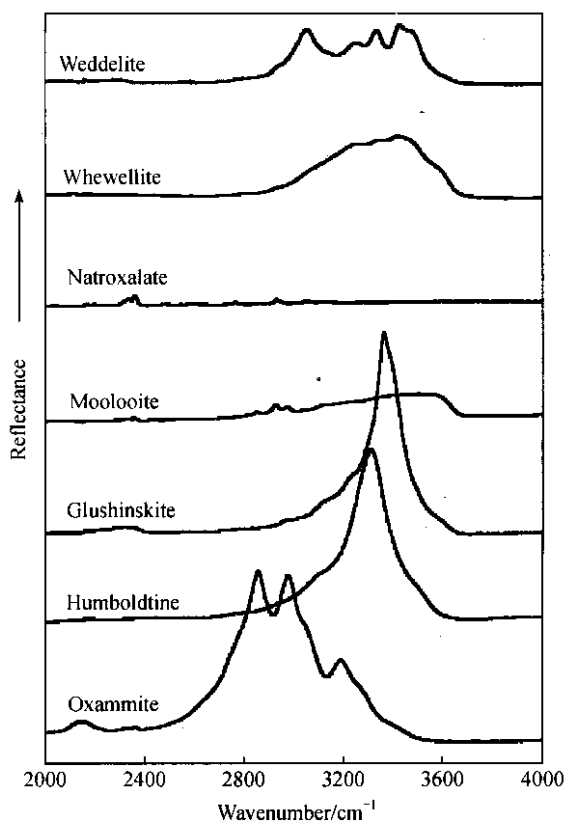


Fig. 7. Patterns of the OH stretching vibrations reflected in the infrared spectra.

3 Conclusions

A suite of natural oxalate minerals have been characterised by both Raman and infrared spectroscopy. Each oxalate mineral has its own characteristic spectrum with the minerals weddelite and whewellite showing strong similarities in their spectrum except for the water OH

stretching region and in the very low wavenumber region. Both natroxalate and moolooite are characterised by the lack of water OH stretching vibrations. The positions of the symmetric and antisymmetric stretching vibrations are characteristic of the particular oxalate and it is suggested that the position of the bands depends on the size and polarity of the cation.

The spectra of the natural oxalates are different. There are a number of reasons for this difference as follows: oxalates may have different structures for example oxammite has a chair-like formation whereas several oxalates are centro-symmetric and planar; the natural oxalates for example moolooite may form polymers with repeat oxalate units; the oxalates may also be a mixture of more than one mineral, for example oxammite may be a mixture of the dihydrate, the anhydrous chemical and a polymer.

If life existed on Mars at some time in the past or even exists in the present time, low life forms such as fungi and lichens may exist. Such organisms may be found in very hostile environments<sup>[38–41]</sup>. Lichens and fungi can control their heavy metal intake through expulsion of metal salts such as oxalates. The presence of these oxalates can be used as a marker for the pre-existence of life. Thus the study of the common natural oxalates is of great importance. The minerals on planets such as Mars may be explored by robotic devices which carry portable spectrometers with possible fibre optics to collect spectral data. The interpretation of the spectra of natural oxalates is important in these types of studies.

**Acknowledgements** Prof. Allan Pring of the South Australian Museum is thanked for the loan of the oxalate minerals, as is also Mr. Ross Pogson of the Australian Museum and Mr. Dermot Henry of Museum Victoria. Prof. Jing Yang also thanks for the visiting fellowship from Queensland University of Technology. The financial and infra-structure support of the Queensland University of Technology Inorganic Materials Research Program is gratefully acknowledged. The Australian Research Council (ARC) is thanked for funding.

## References

1. Arnott, H. J., and Webb, M. A., The structure and formation of calcium oxalate crystal deposits on the hyphae of a wood rot fungus, *Scanning Electron Microsc.*, 1983: 1747–1758.
2. Chisholm, J. E., Jones, G. C., Purvis, O. W., Hydrated copper oxalate, moolooite, in lichens, *Mineralogical Magazine*, 1987, 51: 715–718.
3. Frey-Wyssling, A., Crystallography of the two hydrates of crystalline calcium oxalate in plants, *Am. J. Bot.*, 1981, 68: 130–141.
4. Gadd, G. M., Heterotrophic solubilization of metal-bearing minerals by fungi, *Mineralogical Society Series*, 2000, 9: 57–75.
5. Wadsten, T., Moberg, R., Calcium oxalate hydrates on the surface of lichens, *Lichenologist*, 1985, 17: 239–245.
6. Monje, P. V., Baran, E. J., Characterization of calcium oxalates generated as biominerals in cacti, *Plant Physiology*, 2002, 128: 707–713.
7. Pestaner, J. P., Mullick, F. G., Johnson, F. B. et al., Calcium oxalate crystals in human pathology: molecular analysis with the laser Raman microprobe, *Archives of Pathology & Laboratory Medicine*, 1996, 120: 537–540.
8. Dubernat, J., Pezerat, H., Stacking faults in the dihydrated oxalates of divalent metals of the magnesium series (magnesium, manganese, iron, cobalt, nickel, zinc), *J. Appl. Crystallogr.*, 1974, 7: 387–393.
9. Pezerat, H., Dubernat, J., Lagier, J. P., Structure of magnesium, manganese, iron, cobalt, nickel, and zinc oxalate dihydrates, Existence of stacking faults, *C. R. Acad. Sci., Paris, Ser. C* 1968, 288: 1357–1360.
10. Wilson, M. J., Bayliss, P., Mineral nomenclature: glushinskite, *Mineralogical Magazine*, 1987, 51: 327.
11. Clarke, R. M., Williams, I. R., Moolooite, a naturally occurring hydrated copper oxalate from western Australia, *Mineralogical Magazine*, 1986, 50: 295–298.
12. Rezek, K., Sevcu, J., Civis, S. et al., Humboldtine from Lomnice near Sokolov, western Bohemia, Czechoslovakia, *Casopis pro Mineralogii a Geologii* 1988, 33: 419–424.
13. Manasse, E., Oxalite (humboldtine) from Cape D'Arco (Elba), *Rend. accad. Lincei*, 1911, 19: 138–145.
14. Winchell, H., Benoit, R. J., Taylorite, mascagnite, apthitalite, lecontite, and oxammite from guano, *Am. Mineralogist*, 1951, 36: 590–602.
15. Piterans, A., Indriksone, D., Spricis, A. et al., Biodeterioration of stone historical monuments in Latvia, *Proceedings of the Latvian Academy of Sciences, Section B: Natural, Exact and Applied Sciences*, 1997, 51: 254–260.
16. Del Monte, M., Sabbioni, C., Weddellite on limestone in the Venice [Italy] environment, *Environ. Sci. Technol.*, 1983, 17: 518–522.
17. Del Monte, M., Sabbioni, C., Chemical and biological weathering of an historical building: Reggio Emilia Cathedral, *Science of the Total Environment*, 1986, 50: 165–182.
18. Girbal, J., Prada, J. L., Rocabayera, R. et al., Dating of biodeposits of oxalates at the Arc de Bera in Tarragona, Spain, *Radiocarbon*, 2001, 43: 637–645.
19. Moore, S., Beazley, M. J., McCallum, M. R., et al., Can calcium oxalate residues from lichen activity reflect past climate change? Preprints of Extended Abstracts presented at the ACS National Meeting, American Chemical Society, Division of Environmental Chemistry, 2000, 40: 4–5.



20. Lamprecht, I., Reller, A., Riesen, R. et al., Ca-oxalate films and microbiological investigations of the influence of ancient pigments on the growth of lichens, *Thermogravimetric/thermo-microscopic analyses*, *Journal of Thermal Analysis*, 1997, 49: 1601—1607.
21. Alaimo, R., Montana, G., Study of calcium oxalates bearing patinas of altered calcareous artifacts by BSEI technique, *Neues Jahrbuch fuer Mineralogie, Abhandlungen*, 1993, 165: 143—153.
22. Alessandrini, G., Toniolo, L., Cariati, F. et al., A black paint on the facade of a renaissance building in Bergamo, Italy, *Studies in Conservation*, 1996, 41: 193—204.
23. Moenke, H., Infrared spectrophotometric determination of organic minerals, *Chem. Erde*, 1961, 21: 239—247.
24. Daudon, M., Protat, M. F., Reveillaud, R. J. et al., Infrared spectrometry and Raman microprobe in the analysis of urinary calculi, *Kidney Int.*, 1983, 23: 842—850.
25. Paluszkievicz, C., Galka, M., Kwiatek, W. et al., Renal stone studies using vibrational spectroscopy and trace element analysis, *Biospectroscopy*, 1997, 3: 403—407.
26. Bickley, R. I., Edwards, H. G. M., Rose, S. J., A Raman spectroscopic study of nickel (II) oxalate dihydrate,  $\text{NiC}_2\text{O}_4 \cdot 2\text{H}_2\text{O}$ , and dipotassium bisoxalatonickel (II) hexahydrate,  $\text{K}_2\text{Ni}(\text{C}_2\text{O}_4)_2 \cdot 6\text{H}_2\text{O}$ , *Journal of Molecular Structure*, 1991, 243: 341—350.
27. Chang, H., Huang, P. J., Thermal decomposition of  $\text{cndot H}_2\text{O}$  studied by thermo-raman spectroscopy with TGA/DTA, *Analytical Chemistry*, 1997, 69: 1485—1491.
28. Duval, D., Condrate, R. A., A Raman spectral study of the dehydration of calcium oxalate monohydrate, *Applied Spectroscopy*, 1988, 42: 701—703.
29. Edwards, H. G. M., Farwell, D. W., Jenkins, R. et al., Vibrational Raman spectroscopic studies of calcium oxalate monohydrate and dihydrate in lichen encrustations on Renaissance frescoes, *Journal of Raman Spectroscopy*, 1992, 23: 185—189.
30. Kondilenko, I. I., Korotkov, P. A., Golubeva, N. G. et al., Raman spectrum of an ammonium oxalate monohydrate crystal, *Optika i Spektroskopiya*, 1978, 45: 819—820.
31. Kondratov, O. I., Nikonenko, E. A., Olikov, I. I. et al., Analysis of the vibrational spectrum of nickel oxalate monohydrazinate, *Zhurnal Neorganicheskoi Khimii*, 1985, 30: 2579—2581.
32. Shippey, T. A., Vibrational studies of calcium oxalate monohydrate (whewellite) and an anhydrous phase of calcium oxalate, *Journal of Molecular Structure*, 1980, 63: 157—166.
33. Edwards, H. G. M., Hardman, P. H., A vibrational spectroscopic study of cobalt(II) oxalate dihydrate and the dipotassium bisoxalatocobalt(II) complex, *Journal of Molecular Structure*, 1992, 273: 73—84.
34. Edwards, H. G. M., Lewis, I. R., FT-Raman spectroscopic studies of metal oxalates and their mixtures, *Spectrochimica Acta, Part A: Molecular and Biomolecular Spectroscopy*, 1994, 50A: 1891—1898.
35. Edwards, H. G. M., Farwell, D. W., Rose, S. J. et al., Vibrational spectra of copper(II) oxalate dihydrate,  $\text{CuC}_2\text{O}_4 \cdot 2\text{H}_2\text{O}$ , and dipotassium bis-oxalatocopper(II) tetrahydrate,  $\text{K}_2\text{Cu}(\text{C}_2\text{O}_4)_2 \cdot 4\text{H}_2\text{O}$ , *Journal of Molecular Structure*, 1991, 249: 233—243.
36. Chumaevskii, N. A., Sharopov, O. U., Vibrational spectra and structure of ammonium oxalate monohydrate, *Zhurnal Neorganicheskoi Khimii*, 1988, 33: 1914—1918.
37. Clark, R. J. H., Firth, S., Raman, infrared and force field studies of  $\text{K}_2^{12}\text{C}_2\text{O}_4 \cdot \text{cndot H}_2\text{O}$  and  $\text{K}_2^{13}\text{C}_2\text{O}_4 \cdot \text{cndot H}_2\text{O}$  in the solid state and in aqueous solution, and of  $(\text{NH}_4)_2^{12}\text{C}_2\text{O}_4 \cdot \text{cndot H}_2\text{O}$  and  $(\text{NH}_4)_2^{13}\text{C}_2\text{O}_4 \cdot \text{cndot H}_2\text{O}$  in the solid state, *Spectrochimica Acta, Part A: Molecular and Biomolecular Spectroscopy*, 2002, 58A: 1731—1746.
38. Edwards, H. G. M., Newton, E. M., Russ, J., Raman spectroscopic analysis of pigments and substrata in prehistoric rock art, *Journal of Molecular Structure*, 2000, 550—551: 245—256.
39. Edwards, H. G. M., Russell, N. C., Seaward, M. R. D. et al., Lichen biodeterioration under different microclimates: an FT Raman spectroscopic study, *Spectrochimica Acta, Part A: Molecular and Biomolecular Spectroscopy*, 1995, 51A: 2091—2100.
40. Edwards, H. G. M., Russell, N. C., and Seward, M. R. D., Calcium oxalate in lichen biodeterioration studied using FT-Raman spectroscopy, *Spectrochimica Acta, Part A: Molecular and Biomolecular Spectroscopy*, 1997, 53A: 99—105.
41. Fujita, J., Martell, A. E., Nakamoto, K., Infrared spectra of metal chelate compounds, VI. A normal coordinate treatment of oxalato complexes, *Journal of Chemical Physics*, 1962, 36: 324—338.

(Received March 28, 2003; accepted May 12, 2003)